Frontiers of Optoelectronics (2022) 15:21
https://doi.org/10.1007/s12200-022-00022-7

Frontiers of Optoelectronics

RESEARCH ARTICLE

TCNQ-based organic cocrystal integrated red emission and n-type charge transport

Mengjia Jiang[1] · Shuyu Li[2] · Chun Zhen[1] · Lingsong Wang[1] · Fei Li[1] · Yihan Zhang[1] · Weibing Dong[3] · Xiaotao Zhang[2,3] · Wenping Hu[1,4]

Received: 14 December 2021 / Accepted: 13 January 2022

Abstract
Simultaneously realizing the optical and electrical properties of organic materials is always challenging. Herein, a convenient and promising strategy for designing organic materials with integrated optoelectronic properties based on cocrystal engineering has been put forward. By selecting the fluorene (Flu) and the 7,7′,8,8′-tetracyanoquinodimethane (TCNQ) as functional constituents, the Flu-TCNQ cocrystal prepared shows deep red emission at 702 nm, which is comparable to the commercialized red quantum dot. The highest electron mobility of organic field-effect transistor (OFET) based on Flu-TCNQ is 0.32 $cm^2 V^{-1} s^{-1}$. Spectroscopic analysis indicates that the intermolecular driving force contributing to the co-assembly of Flu-TCNQ is mainly charge transfer (CT) interaction, which leads to its different optoelectronic properties from constituents.

Keywords Organic cocrystal · Charge transfer (CT) · Integrated optoelectronic properties · Red emission · n-type charge transport

1 Introduction

Organic semiconductor materials with characteristics of light weight, flexibility, easy-preparation, large-area solution processing, and low cost have been demonstrated in great applications. Examples are organic field-effect transistor (OFET), organic light-emitting diode (OLED), organic phototransistor (OPT), and organic photovoltaic (OPV) devices [1–6]. Besides single performance optoelectronic materials, organic materials with integrated optoelectronic characteristics are gaining more attention which can serve as candidates for multifunctional optoelectronic devices and integrated circuit fabrication. Examples are the organic light-emitting transistor (OLET) (a device that integrates the functions of OFET and OLED), and pumped organic lasers (EPOLs) [7–10]. In recent years, some organic optoelectronic materials with n/p type charge-carrier mobility and light emission properties have been reported [11–13]. However, most of them exhibit a blue or green emission, and few materials exhibit red emission. In addition, these optoelectronic materials mainly display p-type charge transport behavior [14–16]. Designing and constructing materials with red emission and n-type charge transport is of research significance, but requires a lot of effort. To date, some researchers designed and synthesized materials that combined red emission and n-type charge transfer (CT). Takahiro Kono et al. utilized the efficient fluorophore and small bandgap of dithienylbenzothiadiazole derivative by introducing trifluoromethylphenyl groups, developed an optoelectronic material with red fluorescence and n-type mobility. The benzoselenadiazole and quinoxaline derivatives also exhibit similar optoelectronic properties [17]. Sangyoon Oh et al. investigated the red photoluminescence of an n-type

✉ Xiaotao Zhang
zhangxt@tju.edu.cn

✉ Wenping Hu
huwp@tju.edu.cn

1 Tianjin Key Laboratory of Molecular Optoelectronic Sciences, Department of Chemistry, School of Science, Tianjin University, Tianjin 300072, China

2 Institute of Molecular Aggregation Science, Tianjin University, Tianjin 300072, China

3 Key Laboratory of Resource Chemistry and Eco-Environmental Protection in Qinghai-Tibet Plateau, School of Chemistry and Chemical Engineering, Qinghai Minzu University, Xining 810007, China

4 Joint School of National University of Singapore and Tianjin University, International Campus of Tianjin University, Fuzhou 350207, China

Published online: 09 May 2022

dicyanodistyrylbenzene (DSC-type) derivatives for the first time, and reported the integrated optoelectronic properties of ((2E,2′E)-3,3′-(2,5-*bis*(hexyloxy)-1,4-phenylene) *bis*(2-(5-(4-(trifluoromethyl) phenyl) thiophen-2-yl) acrylonitrile) (Hex-4-TFPTA). They then fabricated the OLET by using the Hex-4-TFPTA as the active layer [18].

Cocrystal is a more ingenious strategy to achieve the integrated optoelectronic properties by noncovalent assembling two or more constituents through intermolecular interactions such as π–π interactions, CT interactions, halogen bonds, and hydrogen bonds [19–21]. The individual constituents can exhibit their inherent properties, and some novel properties also emerge owing to the cooperative effect [22, 23]. Therefore, co-crystallization engenders a promising way for designing and synthesizing the integrated optoelectronic materials with luminescence and charge transport properties, by adjusting donors and acceptors. Yet, many researchers currently focus on constructing materials with the single property of red emission [24, 25] or charge transport [26–28]. Only the Soo Young Park group, designed a series of cocrystals with red emission and charge transport properties through co-assemble molecules that have a 1,4-distyrylbenzene skeleton [29, 30]. The advantages of cocrystals in constructing integrated optoelectronic materials have not been fully utilized.

Herein, the fluorene (Flu) was selected as the donor due to its good luminescence, extended π-conjugated plans, and rich electron properties, which should be an ideal constituent for assembling cocrystals with optoelectronic properties. According to previous reports, the Flu has been used as the luminescence unit to be introduced to special electron-withdrawing group and realized the red emission [31]. As well, 7,7′,8,8′-tetracyanoquinodimethane (TCNQ) was chosen as the electrical building block, a typical n-type semiconductor that can provide a strong electron-withdrawing capacity. Both compositions were easily obtained, avoiding the tedious synthetic routes. The strong CT interaction between donor–acceptor (D–A) pairs is responsible for the co-crystallization. As expected, the binary Flu-TCNQ cocrystal combines the optical and electrical properties of two constituents. Devices fabricated by Flu-TCNQ cocrystal exhibit integrated optoelectronics of deep red luminescence and high n-type charge transport.

2 Experimental and details

2.1 Materials and preparations

Fluorene (Flu, CAS registry no. 86-73-7, 99%) was purchased from Shanghai Aladdin Co., Ltd. (China), and 7,7,8,8,-Tetracyanoquinodimethane (TCNQ, CAS registry no. 1518-16-7, 98%) was purchased from Shanghai TCI Co., Ltd. (China). The dichloromethane solvent and acetonitrile solvents with high performance liquid chromatography (HPLC) grade, were purchased from Shanghai Maclin Co., Ltd. (China).

To grow Flu-TCNQ cocrystals for single-crystal X-ray diffraction characterization, 0.06 mmol Flu and 0.06 mmol TCNQ were dissolved in 10 mL dichloromethane solution at room temperature. The large rod-like Flu-TCNQ cocrystals with good quality were obtained after slow evaporation for five days, and their dark red color was distinct from the pure components (Fig. 1a–c). The Flu-TCNQ microwires for

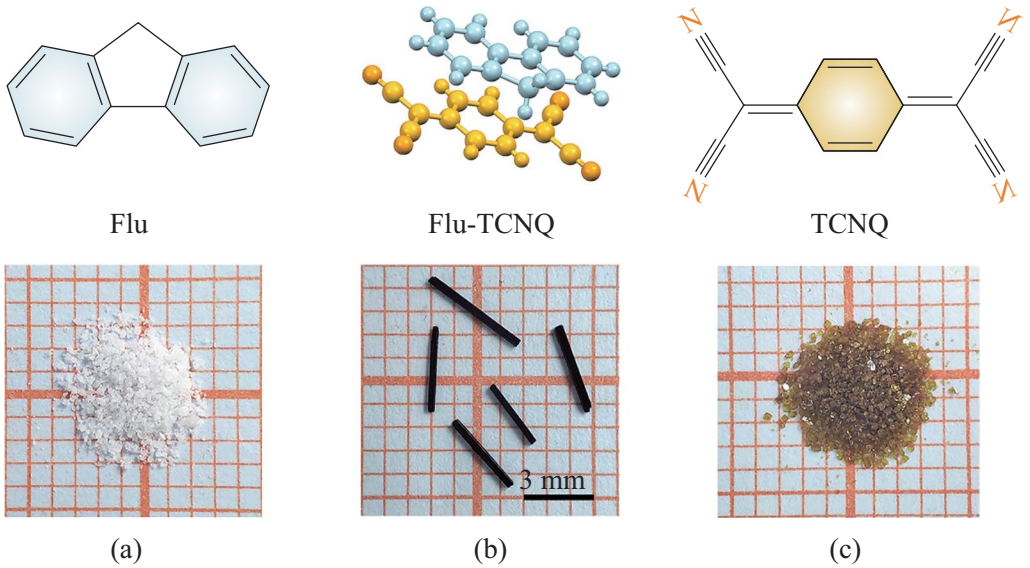

Fig. 1 Optical images of **a** Flu powder, **b** Flu-TCNQ crystal, and **c** TCNQ powder with the chemical structures

OFET fabrication were prepared by the drop-casting method [32]. In a typical experiment, the Flu and TCNQ with a 1:1 ratio was mixed in an acetonitrile solvent. Then the 5−8 μL of mixture solution was immediately dropped onto the modified Si/SiO_2 substrate, and cocrystal microwires were obtained when the solvent in the droplet completely evaporated.

2.2 Device fabrication

To remove impurities, the bare Si wafer (10 mm × 10 mm) was successively washed with pure water, acetone solution, and isopropanol solution in an ultrasonic cleaner for 10 min, respectively. Then the substrate was treated with oxygen plasma for 10 min, followed by the *n*-octadecyl trichlorosilane (OTS) modification via a vapor deposition method. Subsequently, the solution of Flu-TCNQ was dropped onto the prepared substrate to grow microcrystals. The bottom-gate top-contact OFET based on microcrystal was fabricated with stamping Au electrodes by the probe [32, 33]. The measurements of OFET characteristics were performed on Keithley 4200 SCS (USA) and the 6150-probe station, under an ambient condition. The mobility was calculated through

$$I_{DS} = (W/(2L))C_i\mu(V_G - V_{TH})^2, \quad (1)$$

where L and W are the length and width of the channel, respectively; V_G and V_{TH} are the gate voltage and threshold voltage, respectively; C_i is the capacitance per unit area of the insulating layer, μ is the mobility, I_{DS} is the drain current.

2.3 General method

Single-crystal structure data of Flu-TCNQ were collected on a Rigaku Supernova X-ray diffractometer (Japan) with a Cu target at 293 K (40 kV, 30 mA). Powder X-ray diffraction (PXRD) experiment was carried out by a Rigaku SmartLab (Japan) equipment with a Cu target ($\lambda = 1.542$ Å, 40 kV, 200 mA). Thermogravimetric analysis (TGA) was performed on a Mettler Toledo instrument (Switzerland), and the heating temperature was set to rise from 25 °C to 500 °C. The solid-state ultraviolet–visible absorption (UV) measurements were conducted on Shimadzu UV-3600 Plus spectrophotometer (Japan) with an integrating sphere in a diffuse reflection mode. Fourier transform infrared (FTIR) spectrum was obtained on an FTIR spectrometer of Bruker Vertex 70 (Germany). The Raman spectra were acquired on a Renishaw Raman spectrometer (UK) with a 785 nm laser. The electron spin resonance (ESR) test was carried out on a Bruker EMXplus instrument (Switzerland) at room temperature. Photoluminescence (PL) spectroscopies were taken on an Edinburgh FLS1000 instrument (UK). The photoluminescence lifetime (PL lifetime) was measured using a picosecond pulse laser (EPL-340) on the Edinburgh FLS1000. The calculation of average PL lifetime (τ) accords to

$$\tau = \left(B_1\tau_1^2 + B_2\tau_2^2\right)/\left(B_1\tau_1 + B_2\tau_2\right), \quad (2)$$

where τ_1 and τ_2 are the double-exponential values of fitted lifetime, B_1 (2234.0684) and B_2 (947.5385) are the corresponding proportion, respectively. The photoluminescence quantum yield (PLQY) was obtained by using an integrating sphere of the Edinburgh FLS1000 spectrometer (UK).

3 Results and discussion

3.1 Cocrystal structure characterization

To confirm the packing mode and the intermolecular interactions of Flu-TCNQ cocrystal, the single-crystal diffraction was carried out (CCDC 2156827). The crystallographic data denote that the Flu-TCNQ is monoclinic and belongs to the C2/m space group with the lattice parameters of $a = 11.0097(6)$ Å, $b = 13.1035(6)$ Å, $c = 6.7937(3)$ Å, $\alpha = 90°$, $\beta = 103.545(5)°$, $\gamma = 90°$, $V = 952.84(8)$ Å^3 (Additional file 1: Table S1). Figure 2a, b present the mixed packing structure of Flu-TCNQ, wherein the Flu molecule stacks over the center of the TCNQ molecule [34]. In a –D–A–D–A–… column, the Flu and TCNQ pack with a face-to-face mode along the *c* axis, and the D–A distance along the π–π direction is 3.397 Å (Additional file 1: Fig. S1), ensuring the strong intermolecular interaction in Flu-TCNQ [35]. Note that the Flu molecule appears disordered in the Flu-TCNQ cocrystal, because the five-membered ring of Flu occupies two symmetrically positions with the equivalent probability of 50% [36]. Besides, there are multiple C–H…N intermolecular interactions in Flu-TCNQ molecules, as illustrated in Fig. 2c. The distance of C–H…N between TCNQ molecules is 2.687 Å, while that of Flu and TCNQ molecules is 2.582 Å. This hydrogen-bond network not only makes the molecule structure more compact but also promotes the Flu-TCNQ to grow with a rod-like morphology. The packing potential energy was calculated through Mercury software, the energy between the adjacent donor and acceptor molecule is strongest (− 56.0 kJ/mol) (Additional file 1: Fig. S2), revealing the intermolecular driving force for the self-assembly of Flu-TCNQ.

The powder X-ray diffractometer (PXRD) measurements were conducted for a deeper understanding of the cocrystal structure. In Fig. 3a, the PXRD patterns of Flu-TCNQ and the source powders are distinctly different, indicating the Flu-TCNQ is not the simple mixture of two compounds [37]. Additionally, the new finger peaks of cocrystal with sharp shapes and strong intensities suggest the better crystallinity

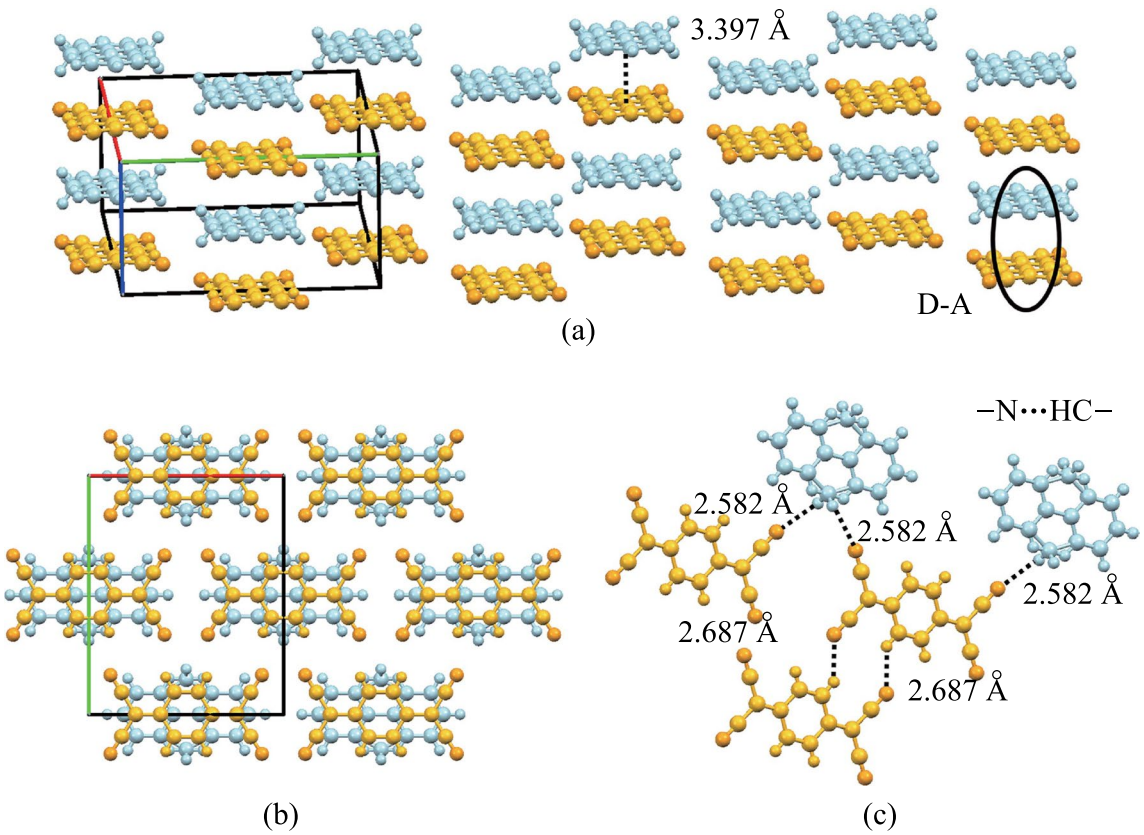

Fig. 2 **a**, **b** Mixed packing structure of Flu-TCNQ (CCDC 2156827). **c** Intermolecular interactions in donor and acceptor molecules of Flu-TCNQ

of the cocrystal. These results of Flu-TCNQ measured by PXRD are in accordance with the simulated data of the CIF file. The thermogravimetric analysis (TGA) was used to evaluate the thermal stability of Flu-TCNQ (Additional file 1: Fig. S3). The smooth curves show that the sublimation points of the pristine Flu and TCNQ are 149 °C and 241 °C, respectively. In the formed cocrystal, the corresponding gradients exhibit higher sublimation points, 199 °C for the Flu component and 251 °C for the TCNQ component. It can be seen that the Flu molecules were completely lost when the temperature was raised to 245 °C. The 54.05% mass loss is consistent with the actual weighting mass ratio of the D–A molecules in Flu-TCNQ. The above analyses indicate that the Flu-TCNQ becomes more stable under co-assembly [38].

3.2 Charge transfer nature and spectra measurements

In consideration of the critical effect of the intermolecular interaction on the crystal properties, a series of spectroscopies were conducted to determine the CT nature and unveil the physicochemical properties of Flu-TCNQ. We measured and analyzed the UV–vis absorption spectra of the as-prepared cocrystal and two constituents (Fig. 3b). It can be observed that the absorption peak of the Flu-TCNQ exhibits significant red-shift and is located at 574 nm, while the absorption peaks of the two pristine components both appear before 500 nm. The absorption band in the region from 510 to 630 nm is assigned as the CT band [39]. In the Fourier transform infrared (FTIR) spectra (Fig. 3c), the peaks of Flu and TCNQ can be recognized from those of Flu-TCNQ, demonstrating the existence of Flu and TCNQ in the as-obtained cocrystal. Specifically, the bands at 3051 cm^{-1} (C–H stretching), 2222 cm^{-1} (C≡N stretching), 1541 cm^{-1} (C=C stretching) in TCNQ are shifted to 3057, 2218, and 1543 cm^{-1} in Flu-TCNQ, respectively, implying the enhanced electron cloud density of the benzene rings in TCNQ molecules [40]. And the band at 733 cm^{-1} in Flu (C–H out-of-plane bending) is shifted to a high wave-number with respect to the 746 cm^{-1} in Flu-TCNQ. These slight movements of peaks are owing to the intermolecular force derived from CT interaction between donors and acceptors. Raman spectra were also recorded to confirm the composition of the cocrystal. As depicted in Additional file 1: Fig. S4, the peaks of Flu-TCNQ are almost the combination of these two constituents. Some small shifts are attributed to

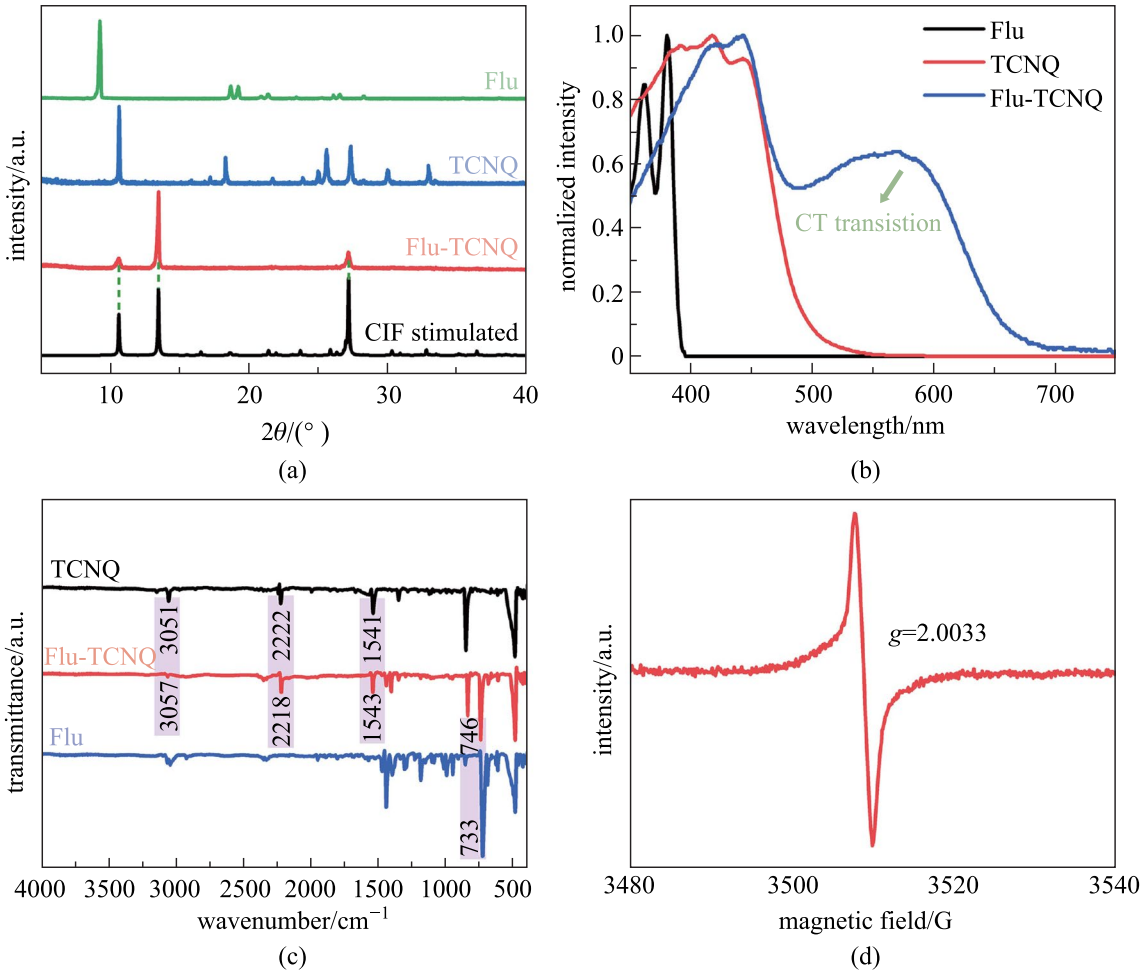

Fig. 3 **a** XRD patterns, **b** UV–Vis absorption spectra, and **c** FTIR spectra of Flu, TCNQ, Flu-TCNQ. **d** ESR spectra of Flu-TCNQ

the polarization and delocalization of electrons between D–A molecules, which facilitate the formation of the CT system in Flu-TCNQ [41]. At the same time, the electron spin resonance spectra (ESR) of Flu-TCNQ was obtained at room temperature (Fig. 3d) The sharp signal that corresponds with a g factor of 2.0033 implies there are unpaired electrons in the ground state, further proving the CT process in the cocrystal [42].

3.3 Optical properties

Driven by the strong intramolecular force, the Flu-TCNQ cocrystal exhibits unique integrated optoelectronic properties. According to the PL spectra, the photophysical properties of Flu-TCNQ were comprehensively researched. Remarkably, compared with the main emission peak of fluorene at 409 nm, the emission peak of Flu-TCNQ is bathochromic shifted to 702 nm (Fig. 4a), implying the CT interaction in the cocrystal, which induces the electron delocalization from Flu to TCNQ [43]. At the same time, the large Stokes shift is 3299 cm^{-1} that is usually less than 3000 cm^{-1} in a single component, and the full width at half-maximum (FWHM) is broadened to 98 nm (Fig. 4b). Besides, the calculated CIE coordinate displays an evident change from Flu (0.16, 0.03) to Flu-TCNQ (0.70, 0.27). (Fig. 4c), demonstrating the successful modulation of luminescent color from blue to the red region by co-assembly. The red color purity is comparable to the (0.71, 0.29) of commercialized red quantum dot [44]. The fluorescence microscope image of Flu-TCNQ microwires with bright red emission is shown in Additional file 1: Fig. S5. Moreover, the fitting PL decay curve with a double-exponential model (fitting constant $X^2 = 1.1493$) was given to better understand the fluorescence properties of the solid-state cocrystal (Fig. 4d). As a result, the average PL lifetime value (τ) is 3.19 ns calculated from the fixed value of $\tau_1 = 2.13$ ns (46.94%) and $\tau_2 = 5.69$ ns (53.06%) [45]. Meanwhile, the solid-state photoluminescence quantum yield (PLQY, ΦF) presents 1.44%.

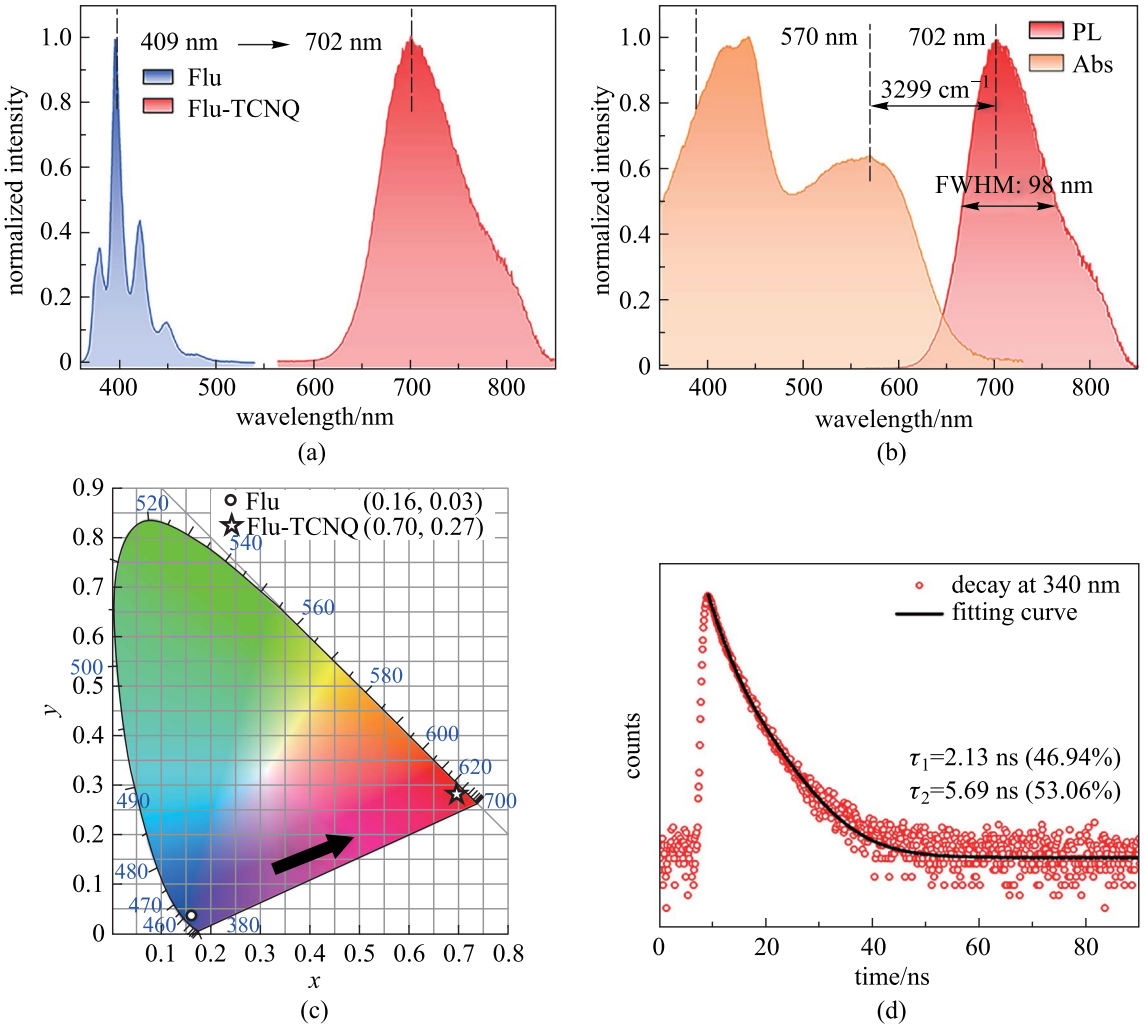

Fig. 4 **a** PL spectra of Flu and Flu-TCNQ. **b** Normalized UV–Vis absorption spectrum and PL spectrum of Flu-TCNQ. **c** CIE 1931 chromaticity diagram and **d** PL decay curve of Flu and Flu-TCNQ

3.4 Electric properties and devices

To investigate the electrical properties of Flu-TCNQ, we fabricated the bottom-gate top-contact OFETs by depositing the microcrystals on Si/SiO_2 substrate (Fig. 5a). Figure 5b, c display the optical and fluorescence microscope images of a typical device based on an individual cocrystal microwire. The transfer and output characteristics of the OFET measured in a hole-enhancement mode are shown in Fig. 5d, e. From the transfer curve, the current between the source and drain electrodes appears at a low gate volt (V_G), and then it increases with the increasing positive V_G, showing a typical n-type charge transport behavior [46]. The highest electron mobility of the OFET extracted from the saturation region can reach 0.32 $cm^2\ V^{-1}\ s^{-1}$ ($V_{DS} = 50$ V), and the on/off ratio is 10^5. Besides, the average electron mobility calculated from 10 OFET devices is 0.25 $cm^2\ V^{-1}\ s^{-1}$. Notably, there may be no direct electron transport channel between the TCNQ molecules due to the mixed packing mode of the Flu-TCNQ. The good electron mobility is mainly attributed to the super-exchange effect in the Flu-TCNQ, where the D–A–D–A cluster provides effective channels for charge transport [47–49]. In our experiment, all the measurements were conducted under the ambient condition, indicating the good air stability of the crystal transistor. The high charge-carrier mobility property endows the Flu-TCNQ with potential application in advanced optoelectronic devices.

4 Conclusion

A Flu-TCNQ cocrystal was prepared with a mixed packing mode and a 1:1 stoichiometric ratio of donor and acceptor. Driven by the strong CT interaction, the Flu-TCNQ exhibits integrated deep red emission and good electron mobility of 0.32 $cm^2\ V^{-1}\ s^{-1}$, which can be considered as

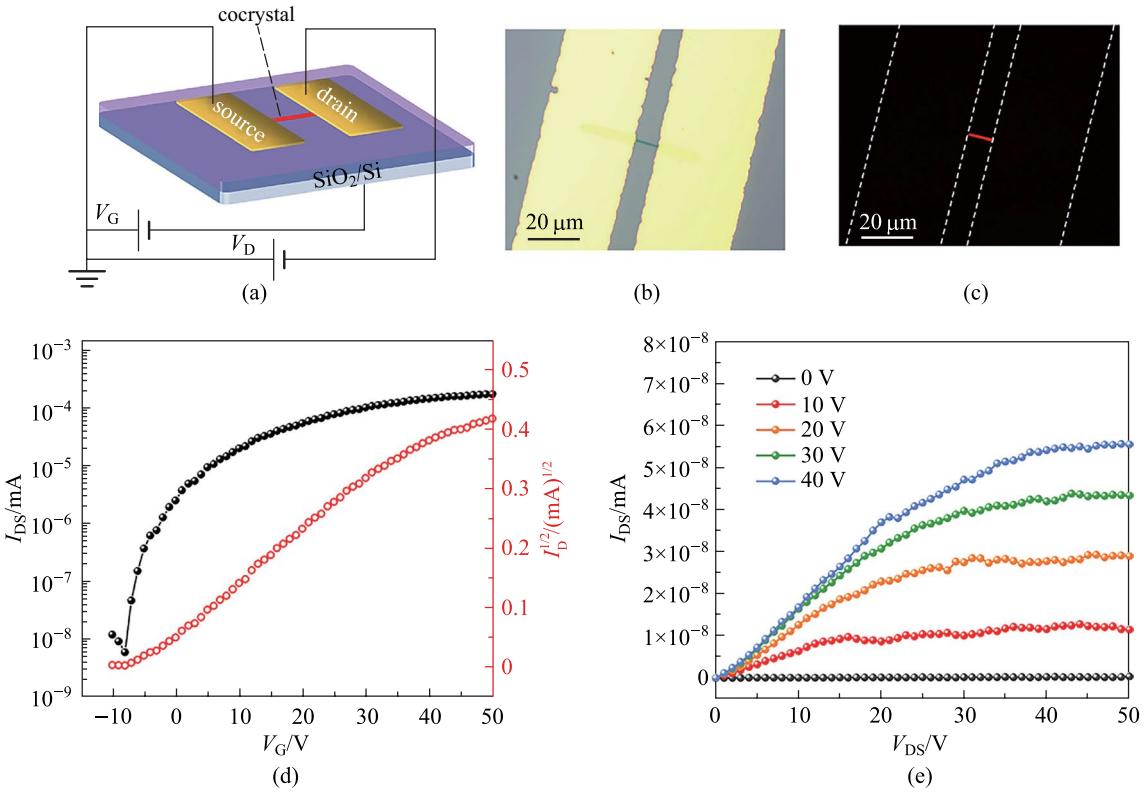

Fig. 5 **a** Schematic diagram of bottom-gate and top-contact OFET device based on a single Flu-TCNQ crystal. **b** Optical microscope image (under visible light) and **c** fluorescence microscope image (under UV) of a typical Flu-TCNQ based OFET. **d** Transfer characteristic of the Flu-TCNQ based OFET at $V_{DS}=50$ V ($L=9.93$ μm, $W=0.44$ μm). **e** Output characteristic of the Flu-TCNQ based OFET scanning from $V_{DS}=0$ to 50 V

a candidate for integrated optoelectronic application. This work is significant for cocrystal engineering and provides guidance in designing and constructing advanced optoelectronic materials. However, there are still difficulties in balancing the optical and electrical properties of the cocrystals. More in-depth and detailed work is still in progress in our laboratory.

Supplementary Information The online version contains supplementary material available at https://doi.org/10.1007/s12200-022-00022-7.

Acknowledgements The authors acknowledge financial support from the National Key R&D Program (No. 2017YFA0204503), the National Natural Science Foundation of China (Grant Nos. 21875158, 51733004, and 91833306), and the Natural Science Foundation of Tianjin City (No. 20JCJQJC00300).

Author contributions ZXT and HWP conceived the project. JMJ synthesized and characterized the cocrystal material including single crystal analysis, optical (U-vis, IR) measurements. ZC conducted the Raman measurements. WLS and ZYH carried out the PL measurements. JMJ and LSY fabricated the OFET. JMJ, LF, and DWB participated in the OFET characteristics. JMJ wrote the paper and drew the schematic diagram. ZXT, HWP, and LSY revised the paper. All authors read and approved the final manuscript.

Declarations

Competing interests The authors declare that they have no competing interests.

References

1. Dong, H., Fu, X., Liu, J., Wang, Z., Hu, W.: 25th anniversary article: key points for high-mobility organic field-effect transistors. Adv. Mater. **25**(43), 6158–6183 (2013)

2. Sirringhaus, H.: 25th anniversary article: organic field-effect transistors: the path beyond amorphous silicon. Adv. Mater. **26**(9), 1319–1335 (2014)
3. Uoyama, H., Goushi, K., Shizu, K., Nomura, H., Adachi, C.: Highly efficient organic light-emitting diodes from delayed fluorescence. Nature **492**(7428), 234–238 (2012)
4. Lee, S.M., Kwon, J.H., Kwon, S., Choi, K.C.: A review of flexible OLEDs toward highly durable unusual displays. IEEE Trans. Electron. Devices **64**(5), 1922–1931 (2017)
5. Yao, Y., Chen, Y., Wang, H., Samorì, P.: Organic photodetectors based on supramolecular nanostructures. SmartMat. **1**(1), e1009 (2020)
6. Brus, V.V., Lee, J., Luginbuhl, B.R., Ko, S.J., Bazan, G.C., Nguyen, T.Q.: Solution-processed semitransparent organic photovoltaics: from molecular design to device performance. Adv. Mater. **31**(30), e1900904 (2019)
7. McCarthy, M.A., Liu, B., Donoghue, E.P., Kravchenko, I., Kim, D.Y., So, F., Rinzler, A.G.: Low-voltage, low-power, organic light-emitting transistors for active matrix displays. Science **332**(6029), 570–573 (2011)
8. Ding, R., An, M.H., Feng, J., Sun, H.B.: Organic single-crystalline semiconductors for light-emitting applications: recent advances and developments. Laser Photonics Rev. **13**(10), 1900009 (2019)
9. Lin, J., Hu, Y., Lv, Y., Guo, X., Liu, X.: Light gain amplification in microcavity organic semiconductor laser diodes under electrical pumping. Sci. Bull. **62**(24), 1637–1638 (2017)
10. Chénais, S., Forget, S.: Recent advances in solid-state organic lasers. Polym. Int. **61**(3), 390–406 (2012)
11. Qin, Z., Gao, H., Dong, H., Hu, W.: Organic light-emitting transistors entering a new development stage. Adv. Mater. **33**(31), e2007149 (2021)
12. Liu, J., Zhang, H., Dong, H., Meng, L., Jiang, L., Jiang, L., Wang, Y., Yu, J., Sun, Y., Hu, W., Heeger, A.J.: High mobility emissive organic semiconductor. Nat. Commun. **6**(1), 10032 (2015)
13. Melucci, M., Favaretto, L., Zambianchi, M., Durso, M., Gazzano, M., Zanelli, A., Monari, M., Lobello, M.G., De Angelis, F., Biondo, V., Generali, G., Troisi, S., Koopman, W., Toffanin, S., Capelli, R., Muccini, M.: Molecular tailoring of new thieno(bis) imide-based semiconductors for single layer ambipolar light emitting transistors. Chem. Mater. **25**(5), 668–676 (2013)
14. Deng, J., Xu, Y., Liu, L., Feng, C., Tang, J., Gao, Y., Wang, Y., Yang, B., Lu, P., Yang, W., Ma, Y.: An ambipolar organic field-effect transistor based on an AIE-active single crystal with a high mobility level of 2.0 $cm^2 \cdot V^{-1} \cdot s^{-1}$. Chem. Commun. **52**(12), 2647 (2016)
15. Yomogida, Y., Takenobu, T., Shimotani, H., Sawabe, K., Bisri, S.Z., Yamao, T., Hotta, S., Iwasa, Y.: Green light emission from the edges of organic single-crystal transistors. Appl. Phys. Lett. **97**(17), 173301 (2010)
16. Liu, D., De, J., Gao, H., Ma, S., Ou, Q., Li, S., Qin, Z., Dong, H., Liao, Q., Xu, B., Peng, Q., Shuai, Z., Tian, W., Fu, H., Zhang, X., Zhen, Y., Hu, W.: Organic laser molecule with high mobility, high photoluminescence quantum yield, and deep-blue lasing characteristics. J. Am. Chem. Soc. **142**(13), 6332–6339 (2020)
17. Kono, T., Kumaki, D., Nishida, J., Sakanoue, T., Kakita, M., Tada, H., Tokito, S., Yamashita, Y.: High-performance and light-emitting n-type organic field-effect transistors based on dithienylbenzothiadiazole and related heterocycles. Chem. Mater. **19**(6), 1218–1220 (2007)
18. Oh, S., Kim, J.H., Park, S.K., Ryoo, C.H., Park, S.Y.: Fabrication of pixelated organic light-emitting transistor (OLET) with a pure red-emitting organic semiconductor. Adv. Opt. Mater. **7**(23), 1901274 (2019)
19. Zhu, W., Dong, H., Zhen, Y., Hu, W.: Challenges of organic "cocrystals." Sci. China Mater. **58**(11), 854–859 (2015)
20. Huang, Y., Wang, Z., Chen, Z., Zhang, Q.: Organic cocrystals: beyond electrical conductivities and field-effect transistors (FETs). Angew Chem. Int. Ed. **58**(29), 9696–9711 (2019)
21. Zhang, J., Xu, W., Sheng, P., Zhao, G., Zhu, D.: Organic donor–acceptor complexes as novel organic semiconductors. Acc. Chem. Res. **50**(7), 1654–1662 (2017)
22. Sun, L., Yang, F., Zhang, X., Hu, W.: Stimuli-responsive behaviors of organic charge transfer cocrystals: recent advances and perspectives. Mater. Chem. Front. **4**(3), 715–728 (2020)
23. Sun, L., Wang, Y., Yang, F., Zhang, X., Hu, W.: Cocrystal engineering: a collaborative strategy toward functional materials. Adv. Mater. **31**(39), e1902328 (2019)
24. Wang, Y., Wu, H., Li, P., Chen, S., Jones, L.O., Mosquera, M.A., Zhang, L., Cai, K., Chen, H., Chen, X.Y., Stern, C.L., Wasielewski, M.R., Ratner, M.A., Schatz, G.C., Stoddart, J.F.: Two-photon excited deep-red and near-infrared emissive organic co-crystals. Nat. Commun. **11**(1), 4633 (2020)
25. Bhowal, R., Biswas, S., Thumbarathil, A., Koner, A.L., Chopra, D.: Exploring the relationship between intermolecular interactions and solid-state photophysical properties of organic co-crystals. J. Chem. Phys. **123**(14), 9311–9322 (2019)
26. Black, H.T., Perepichka, D.F.: Crystal engineering of dual channel p/n organic semiconductors by complementary hydrogen bonding. Angew Chem. Int. Ed. **53**(8), 2138–2142 (2014)
27. Liu, H., Liu, Z., Jiang, W., Fu, H.: Tuning the charge transfer properties by optimized donor–acceptor cocrystal for FET applications: from P type to N type. J. Solid State Chem. **274**, 47–51 (2019)
28. Liang, Y., Qin, Y., Chen, J., Xing, W., Zou, Y., Sun, Y., Xu, W., Zhu, D.: Band engineering and majority carrier switching in isostructural donor–acceptor complexes DPTTA-F_XTCNQ crystals ($X = 1, 2, 4$). Adv. Sci. **7**(3), 1902456–1902464 (2019)
29. Park, S.K., Varghese, S., Kim, J.H., Yoon, S.J., Kwon, O.K., An, B.K., Gierschner, J., Park, S.Y.: Tailor-made highly luminescent and ambipolar transporting organic mixed stacked charge-transfer crystals: an isometric donor–acceptor approach. J. Am. Chem. Soc. **135**(12), 4757–4764 (2013)
30. Park, S.K., Kim, J.H., Ohto, T., Yamada, R., Jones, A.O.F., Whang, D.R., Cho, I., Oh, S., Hong, S.H., Kwon, J.E., Kim, J.H., Olivier, Y., Fischer, R., Resel, R., Gierschner, J., Tada, H., Park, S.Y.: Highly luminescent 2D-type slab crystals based on a molecular charge-transfer complex as promising organic light-emitting transistor materials. Adv. Mater. **29**(36), 1701346 (2017)
31. Chiang, C.L., Wu, M.T., Dai, D.C., Wen, Y.S., Wang, J.K., Chen, C.T.: Red-emitting fluorenes as efficient emitting hosts for non-doped, organic red-light-emitting diodes. Adv. Funct. Mater. **15**(2), 231–238 (2005)
32. Sun, L., Zhu, W., Yang, F., Li, B., Ren, X., Zhang, X., Hu, W.: Molecular cocrystals: design, charge-transfer and optoelectronic functionality. Phys. Chem. Chem. Phys. **20**(9), 6009–6023 (2018)
33. Jiang, L., Gao, J., Wang, E., Li, H., Wang, Z., Hu, W., Jiang, L.: Organic single-crystalline ribbons of a rigid "H"-type anthracene derivative and high-performance, short-channel field-effect transistors of individual micro/nanometer-sized ribbons fabricated by an "organic ribbon mask" technique. Adv. Mater. **20**(14), 2735–2740 (2008)
34. Wang, W., Luo, L., Sheng, P., Zhang, J., Zhang, Q.: Multifunctional features of organic charge-transfer complexes: advances and perspectives. Chemistry (Weinheim an der Bergstrasse, Germany) **27**(2), 464–490 (2021)
35. Qin, Y., Cheng, C., Geng, H., Wang, C., Hu, W., Xu, W., Shuai, Z., Zhu, D.: Efficient ambipolar transport properties in alternate stacking donor–acceptor complexes: from experiment to theory. Phys. Chem. Chem. Phys. **18**(20), 14094–14103 (2016)
36. Croce, G., Arrais, A., Diana, E., Civalleri, B., Viterbo, D., Milanesio, M.: The interpretation of the short range disorder in the

fluorene TCNE crystal structure. Int. J. Mol. Sci. **5**(3), 93–100 (2004)
37. Zhang, J., Geng, H., Virk, T.S., Zhao, Y., Tan, J., Di, C.A., Xu, W., Singh, K., Hu, W., Shuai, Z., Liu, Y., Zhu, D.: Sulfur-bridged annulene-TCNQ co-crystal: a self-assembled "molecular level heterojunction" with air stable ambipolar charge transport behavior. Adv. Mater. **24**(19), 2603–2607 (2012)
38. Usman, R., Khan, A., Sun, H., Wang, M.: Study of charge transfer interaction modes in the mixed donor–acceptor cocrystals of pyrene derivatives and TCNQ: a combined structural, thermal, spectroscopic, and hirshfeld surfaces analysis. J. Solid State Chem. **266**, 112–120 (2018)
39. Wakahara, T., Nagaoka, K., Nakagawa, A., Hirata, C., Matsushita, Y., Miyazawa, K., Ito, O., Wada, Y., Takagi, M., Ishimoto, T., Tachikawa, M., Tsukagoshi, K.: One-dimensional fullerene/porphyrin cocrystals: near-infrared light sensing through component interactions. ACS Appl. Mater. Interfaces **12**(2), 2878–2883 (2020)
40. Wang, Y., Zhu, W., Du, W., Liu, X., Zhang, X., Dong, H., Hu, W.: Cocrystals strategy towards materials for near-infrared photothermal conversion and imaging. Angew Chem. Int. Ed. **57**(15), 3963–3967 (2018)
41. Liang, Y., Xing, W., Liu, L., Sun, Y., Xu, W., Zhu, D.: Charge transport behaviors of a novel 2:1 charge transfer complex based on coronene and HAT$(CN)_6$. Org. Electron. **78**, 105608 (2020)
42. Mandal, A., Swain, P., Nath, B., Sau, S., Mal, P.: Unipolar to ambipolar semiconductivity switching in charge transfer cocrystals of 2,7-di-tertbutylpyrene. CrystEngComm. **21**(6), 981–989 (2019)
43. Ye, H., Liu, G., Liu, S., Casanova, D., Ye, X., Tao, X., Zhang, Q., Xiong, Q.: Molecular-barrier-enhanced aromatic fluorophores in cocrystals with unity quantum efficiency. Angew Chem. Int. Ed. **57**(7), 1928–1932 (2018)
44. Dai, X., Zhang, Z., Jin, Y., Niu, Y., Cao, H., Liang, X., Chen, L., Wang, J., Peng, X.: Solution-processed, high-performance light-emitting diodes based on quantum dots. Nature **515**(7525), 96–99 (2014)
45. Wu, H., Sun, Y., Sun, L., Wang, L., Zhang, X., Hu, W.: Deep insight into the charge transfer interactions in 1,2,4,5-tetracyanobenzene-phenazine cocrystal. Chin. Chem. Lett. **32**(10), 3007–3010 (2021)
46. Tsutsumi, J., Matsuoka, S., Inoue, S., Minemawari, H., Yamada, T., Hasegawa, T.: N-type field-effect transistors based on layered crystalline donor–acceptor semiconductors with dialkylated benzothienobenzothiophenes as electron donors. J. Mater. Chem. C Mater. Opt. Electron. Dev. **3**(9), 1976–1981 (2015)
47. Geng, H., Zhu, L., Yi, Y., Zhu, D., Shuai, Z.: Superexchange induced charge transport in organic donor–acceptor cocrystals and copolymers: a theoretical perspective. Chem. Mater. **31**(17), 6424–6434 (2019)
48. Geng, H., Zheng, X., Shuai, Z., Zhu, L., Yi, Y.: Understanding the charge transport and polarities in organic donor–acceptor mixed-stack crystals: molecular insights from the superexchange couplings. Adv. Mater. **27**(8), 1443–1449 (2015)
49. Zhu, L., Geng, H., Yi, Y., Wei, Z.: Charge transport in organic donor–acceptor mixed-stack crystals: the role of nonlocal electron–phonon couplings. Phys. Chem. Chem. Phys. **19**(6), 4418–4425 (2017)

Mengjia Jiang is a master's student at Tianjin Key Laboratory of Molecular Optoelectronic Sciences, Tianjin University, China. She majors in chemistry. Her current research focuses on functional organic cocrystals.

Shuyu Li is pursuing a Ph.D. at Institute of Molecular Aggregation Science, Tianjin University, China. She mainly works on the electrical properties of organic cocrystal materials.

Chun Zhen is currently working toward a master's degree at Tianjin Key Laboratory of Molecular Optoelectronic Sciences, Tianjin University, China. Her research interests focus on the photoelectrical properties of organic cocrystals.

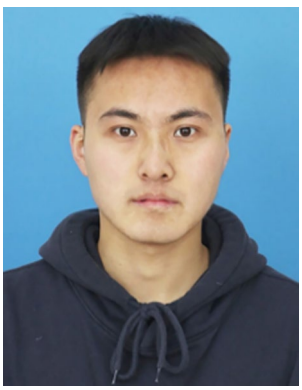

Lingsong Wang is pursuing a master's degree at Tianjin Key Laboratory of Molecular Optoelectronic Sciences, Tianjin University, China. He focuses on the design, synthesis, and application of organic cocrystals.

Fei Li is a master's student at Tianjin Key Laboratory of Molecular Optoelectronic Sciences, Tianjin University, China. He mainly works on the design and application of organic functional materials.

Yihan Zhang is a master's student at Tianjin Key Laboratory of Molecular Optoelectronic Sciences, Tianjin University, China. Her research interests are organic crystal materials and optoelectronic devices.

Weibing Dong is an associate professor in School of Chemistry and Chemical Engineering at Qinghai Minzu University, China. He obtained his B.S. degree (2004) from Taiyuan University of Technology, China; M.S. degree (2007) in Pharmaceutical Engineering, and Ph.D. degree (2010) in Chemical Engineering both from Tianjin University, China. His current research focuses on crystal engineering and Industrial crystallization.

Xiaotao Zhang is a professor at Institute of Molecular Aggregation Science, Tianjin University, China. He received his Ph.D. degree from Institute of Chemistry, Chinese Academy of Sciences, China in 2012 after he got his M.Sc. degree (2007) at Zhejiang University, China. His research work includes the design and synthesis of novel organic semiconductors, the fabrication, and characterization of organic optoelectronic devices.

Wenping Hu is a professor of School of Science, Tianjin University, China. He got his M.S. degree from Institute of Metal Research, Chinese Academy of Sciences (ICCAS), China in 1996 and Ph.D. degree from Institute of Chemistry, CAS in 1999. Then he joined Osaka University and Stuttgart University as a research fellow of Japan Society for the Promotion of Sciences and Alexander von Humboldt Fellowship, respectively. In 2003 he worked in Nippon Telephone and Telegraph (NTT), and then joined ICCAS again as a full professor. He served as a Visiting Scholar at Department of Chemistry, Stanford University in 2007, a Visiting Professor at Department of Chemistry, National University of Singapore in 2013. He worked as the dean of School of Science, Tianjin University in 2013 and was promoted to vice president for foreign affairs and science development in 2016. He focuses on organic semiconductors, crystals, and devices for decades. He has published ~500 peer-reviewed papers with citations over 27000 times (H index = 82).